Geology of the Hoidas Lake Area, Ena Domain, Northwestern Saskatchewan

S.E. Harvey, I. Young [1], and G. Billingsley [1]

Harvey, S.E., Young, I., and Billingsley, G. (2002): Geology of the Hoidas Lake area, Ena Domain, northwestern Saskatchewan; *in* Summary of Investigations 2002, Volume 2, Saskatchewan Geological Survey, Sask. Industry Resources, Misc. Rep. 2002-4.2, CD-ROM, Paper C-2, 13p.

Abstract

The structurally controlled Hoidas Lake rare-earth element (REE) deposit is near the eastern edge of the Ena Domain, 60 km northeast of Uranium City, and 3 km west of the Black Bay Fault. Current research on the deposit and the surrounding area included 1:10 000 scale regional mapping, more detailed 1:2 500 scale property mapping on a cut grid, and the logging of NQ core from five holes through the deposit. The purpose of the work was to establish a regional framework for the REE mineralization.

In the 1950s, allanite showings were discovered along a strike length of 10 km in the Nisikkatch-Hoidas lakes area. Grab samples from the northwest side of Hoidas Lake contained up to 7% Ce, 6% La, 2% Th, and total rare-earth element concentrations up to 12%. In the late 1990s, the main Jak zone was systematically trenched and sampled and then tested by diamond drilling in 2001. Intervals up to 6.9 m thick contained 4.4% total rare-earth oxides, and metallurgical work indicated that 95 to 99% of the REEs could be extracted using readily available, non-toxic reagents to leach the elements.

Regionally, granitic and tonalitic gneisses dominate and intrude amphibolite that exhibits local compositional layering (S_0). Late intrusive rocks include garnetiferous dioritic gneiss and granitic pegmatite. Early D_1 deformation produced isoclinal folds parallel to a locally preserved S_1 foliation. This was overprinted by northeast-trending D_2 shearing and tight to isoclinal folding. The intensity of the S_2 foliation is highly variable, ranging from weakly gneissic west of Hoidas Lake to mylonite (<500 m wide) coincident with the lake, and in local narrow zones to the east. Rare kinematic indicators suggest oblique-dextral movement in the ductile shear zones. Late faults and fractures trend in three general directions: east, northeast, and southeast. The northeast-trending set appears to overprint older D_2 shear structures and is probably related to the Black Bay Fault.

REE minerals are in a 60m wide system of veins in northeast-trending fractures/faults; they have a drill-defined strike length of at least 475 m. Individual veins are up to 5 m wide and have a variably developed mineral zonation defined by two main phases: a pyroxene-rich zone of clinopyroxene, scapolite, allanite and amphibole; and an apatite-rich zone of apatite and allanite. The paragenesis of these veins remains ambiguous and requires further study, however, initial work suggests that they may be the result of metasomatism/metamorphism of a pyroxene-rich ultramafic to lamprophyric vein/dyke system that intruded northeast-trending brittle-ductile to brittle fault/fracture zones. An influx of calcium-enriched fluids during/after initial vein emplacement resulted in production of pyroxene-scapolite-rich and apatite-rich rocks. Abundant late, thin peridotitic and pyroxenitic dykes and lenses near the Black Bay Fault and the Tazin Lake Fault to the southwest might be associated with those which host the Hoidas Lake deposit and may be a target for future exploration.

***Keywords**: Precambrian, structure, veins, rare-earth elements, REE, Ena Domain, economic geology, clinopyroxene veins, apatite veins, Black Bay Fault, allanite.*

1. General

A 1:10 000scale geological mapping program covering a 25 km^2 area centered on Hoidas Lake was conducted in the region west of the Black Bay Fault and north of the Tazin River Fault (Figure 1; part of NTS map sheet 74O/13). Mapping, during a two-week period in the summer of 2002, was undertaken to establish the regional context of the Hoidas Lake rare-earth element (REE) deposit. Additional work included 1:2 500 scale mapping of the main zone (Jak), and the logging of five core from NQ drill holes covering a 300 m strike length of the Jak zone. Previous work in the area included reconnaissance-scale mapping (Alcock, 1936) followed by 1"=1 mile scale mapping by

[1] Great Western Minerals Group Ltd., P.O. Box 69, Saskatoon, SK S7K 3K1.

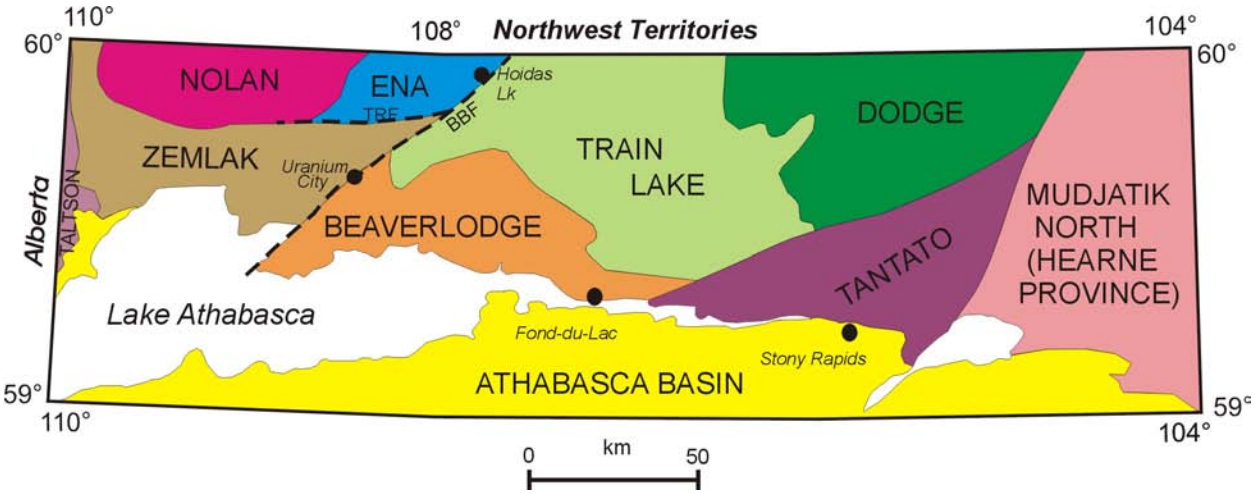

Figure 1 - Location map showing lithotectonic domains in northwestern Saskatchewan. BBF=Black Bay Fault; TRF=Tazin River Fault.

Saskatchewan Department of Mineral Resources (74O/13W; Koster, 1965a). The area is also included in a subsequent 1:250 000 scale geological compilation map of the Fond-du-Lac area (Slimmon, 1989).

2. General Geology of the Hoidas Lake Area

Hoidas Lake is 60 km northeast of Uranium City and lies in the eastern part of the Ena Domain in the Rae Province (Figure 1). The southeastern limit of the Ena Domain is marked by the long-lived Black Bay Fault, 3 km east of Hoidas Lake. The area has been affected by multiple thermotectonic events, including those presumed to be related to the Thelon and/or Trans-Hudson orogenies.

Granulite facies quartzofeldspathic gneisses of dioritic to granitic composition dominate the Ena Domain, formerly termed the Ena Lake complex (Macdonald, 1983) and the Northern complex (Koster, 1965a, 1965b). Subordinate amphibolitic rocks occur in narrow belts and as schlieren within granitoid rocks. Locally, to the northwest are garnet-bearing quartzofeldspathic rocks of possible metasedimentary origin.

Two main northeast-trending units are separated by a 200 to 500 m wide mylonite zone coincident with Hoidas Lake (Figure 2). Granitic and lesser tonalitic gneiss dominate west of Hoidas Lake, whereas to the east, tonalitic gneiss is the main rock type with granitic gneiss being subordinate. The rocks range from near massive gneiss in the west to moderately strained gneiss containing local high-strain zones approaching the Black Bay Fault in the east.

a) Amphibolitic Gneiss (Mv)

Amphibolite is commonly in thin (<100 m), discontinuous belts and as inclusions and schlieren within the granitoid gneisses (Figure 2). Most outcrops include 5 to 20% leucosome which helps to define gneissosity. The amphibolitic gneiss typically weathers light to dark grey and is fine to medium grained. It is composed of 30 to 50% hornblende, 40 to 60% plagioclase (An_{48-60}), 0 to 10% variably chloritized biotite, 0 to 10% clinopyroxene, along with trace apatite and sphene. Parallel alignment of the long axis of hornblende and biotite define the foliation. Alternation of feldspar- and hornblende-rich layers, in some outcrops, may be indicative of transposed primary layering (S_0). Plagioclase is partially to completely replaced by sericite.

b) Granitic Gneiss (Gr)

Pink to red, medium- to fine-grained granitic gneiss varies from near massive and medium-grained in the west to fine- to medium-grained gneissic equivalents towards Hoidas Lake in the east (Figure 2). It is the dominant lithology west of Hoidas Lake, whereas to the east, it is restricted to narrow (<300 m), semi-continuous belts. The unit is commonly intermixed with, and locally crosscuts, amphibolitic gneiss, which comprises 5 to 50% of the outcrop (Figure 3).

The granitic gneiss is composed of 35 to 70% microcline, 20 to 45% quartz, 7 to 35% plagioclase, 0 to 10% biotite, 0 to 10% hornblende, 0 to 7% clinopyroxene, trace to 3% opaque minerals, and trace to 2% apatite. Allanite is a common accessory mineral. Total mafic content in the unit ranges from 3 to 15%. The unit is non- to weakly

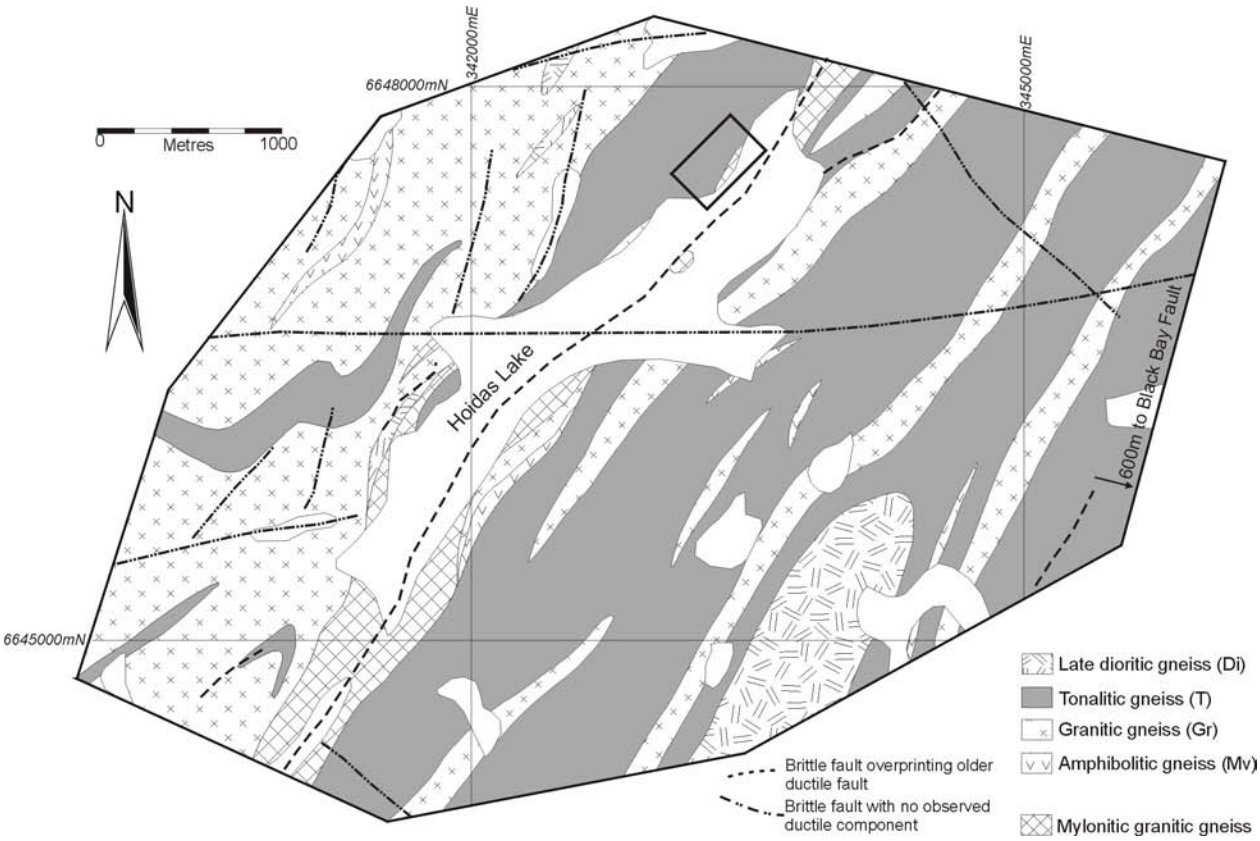

Figure 2 - Simplified geological map of the Hoidas Lake area. Rectangle outlines the extent of the main zone (Jak) grid. UTM coordinates are in NAD27.

magnetic, with local moderately magnetic areas. The degree of replacement of plagioclase by sericite, associated with hematite dusting, ranges from slight along grain boundaries to pervasive and is commonly related to proximity to late fractures. Biotite grains, which help to define the foliation, have been variably replaced by chlorite. Mylonitic varieties, observed along the western, and southern shores of Hoidas Lake, exhibit strong quartz ribboning.

c) Tonalitic Gneiss (T)

Grey to pink, medium- to locally fine-grained tonalitic gneiss occurs throughout the area, and is the dominant unit east of Hoidas Lake (Figure 2). Relatively homogeneous, medium-grained tonalite grades into more gneissic, and locally mylonitic equivalents eastwards. As in the granitic gneisses, amphibolitic schlieren are also common comprising 10 to 30% of most outcrops. The tonalitic gneiss is composed of 30 to 50% plagioclase, 15 to 35% quartz, 5 to 20% biotite, 0 to 15% potassium feldspar, 0 to 25% hornblende, 0 to 15% orthopyroxene, 0 to 5% clinopyroxene, and trace to 6% opaque minerals. Orthopyroxene is typically hypersthene, although an iron-rich variety, possibly ferrosilite, is not uncommon. In contrast to the granitic gneiss unit, the tonalitic rocks are moderately to strongly magnetic.

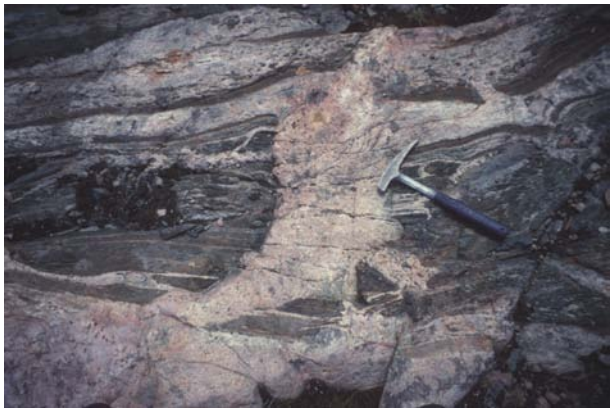

Figure 3 - Amphibolitic gneiss intruded by, and intermixed with, granitic gneiss sheets. Both units are crosscut by a younger granitic pegmatite.

d) Late Garnetiferous Dioritic Gneiss (Di)

A dark green to black, medium- to coarse-grained dioritic intrusive, more than 500 m in diameter is in the southeast; smaller similar intrusions are observed

throughout the area. The intrusions have massive cores but are progressively foliated towards their margins. Limited thin section examination revealed that this rock is composed of 45 to 70% hornblende locally replaced by chlorite, 35 to 50% variably sericitized plagioclase (An_{43-50}), 0 to 3% biotite, 0 to 3% orthopyroxene, and 2 to 15% fine to very coarse (up to 3 cm) garnet porphyroblasts (Figure 4). Accessory minerals include apatite, biotite, chlorite, allanite, and opaque minerals.

e) Pegmatite and Pegmatitic Granite

Pink, medium-grained to pegmatitic granite is common, constituting 5 to 40% of most outcrops. The pegmatites are typically massive, homogeneous, and straight-sided veins that crosscut all previously described units (Figure 3). The veins generally trend to the northeast and are concordant to locally discordant relative to the main S_2 fabric.

3. Structural Geology

Hoidas Lake area has been subjected to several phases of folding and faulting. Folding is predominantly recognized on the outcrop scale. The main structural fabric trends northeasterly and is associated with tight to isoclinal folds and locally a mineral stretching lineation. The presence of both orthopyroxene and clinopyroxene in the same rock indicates that granulite facies metamorphic conditions in excess of 750ºC were attained (Bucher and Frey, 1994). Highly altered white rims around garnet grains in late dioritic gneiss (Figure 4) imply decompression reactions possibly attributed to a lower-grade metamorphic event.

Figure 4 - Garnet porphyroblasts in a moderately foliated late diorite. Note the thin white (decompression) reaction rims around garnets.

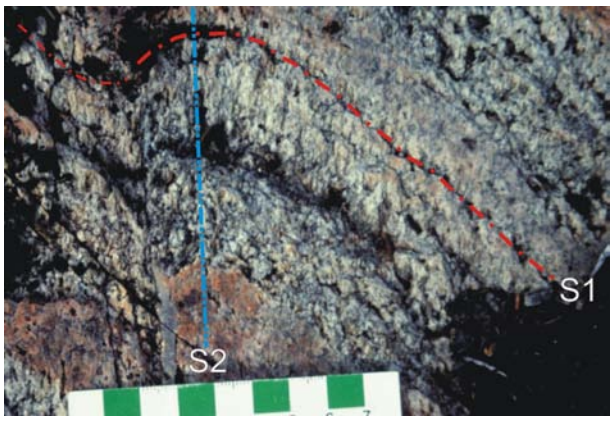

Figure 5 - Early leucosome defining the S_1 gneissosity overprinted by a crosscutting S_2 foliation in granitic gneiss at the south end of Hoidas Lake. Note that S_2 parallels a small sinistral shear zone.

a) D_1 Deformation

Apart from transposed compositional layering (S_0) locally recognized in the older amphibolite, the combined effects of deformation and metamorphism have obliterated primary features. First-generation structures are best preserved in amphibolite and include a rare S_1 gneissosity, which is partially defined by leucosomal layers derived during upper amphibolite to granulite facies partial melting, and the parallel alignment of the long axis of mafic minerals. The S_1 foliation is axial planar to rare F_1 isoclinal folds.

b) D_2 Deformation

D_2 formed the dominant northeast structural grain and is probably associated with ductile shearing of the Black Bay Shear Zone. The S_1 fabric has been variably overprinted by the regionally dominant S_2 foliation, which ranges from weak to mylonitic. Where observed, S_1 is typically rotated into parallelism with S_2 resulting in the regional foliation being defined as a composite $S_0/S_1/S_2$ fabric. Locally, however, the S_2 foliation is observed overprinting the predominantly leucosomally-defined S_1 gneissosity (Figures 5). The S_2 foliation is defined by the parallel alignment of the long axes of mafic minerals including biotite, hornblende, and chlorite. It strikes northeast and dips steeply to the southeast or less commonly to the northwest (Figure 6a). On a stereonet plot of poles to the foliation plane the two maxima may define the limbs of tight F_2 folds (Figure 6a). The foliation is axial planar to tight to isoclinal northeast-southwest-trending doubly plunging F_2 folds (Figure 6b and 7). The folds are typically symmetric with z-asymmetry rare.

There is a recognizable increase in the intensity of the S_2 fabric towards the eastern margin of the map area. In the west, heterogeneously developed, centimeter-scale D_2 shear zones (Figure 6c) are typically infilled with pegmatite. They appear to form a conjugate set comprising north-trending sinistral shears and northeast-

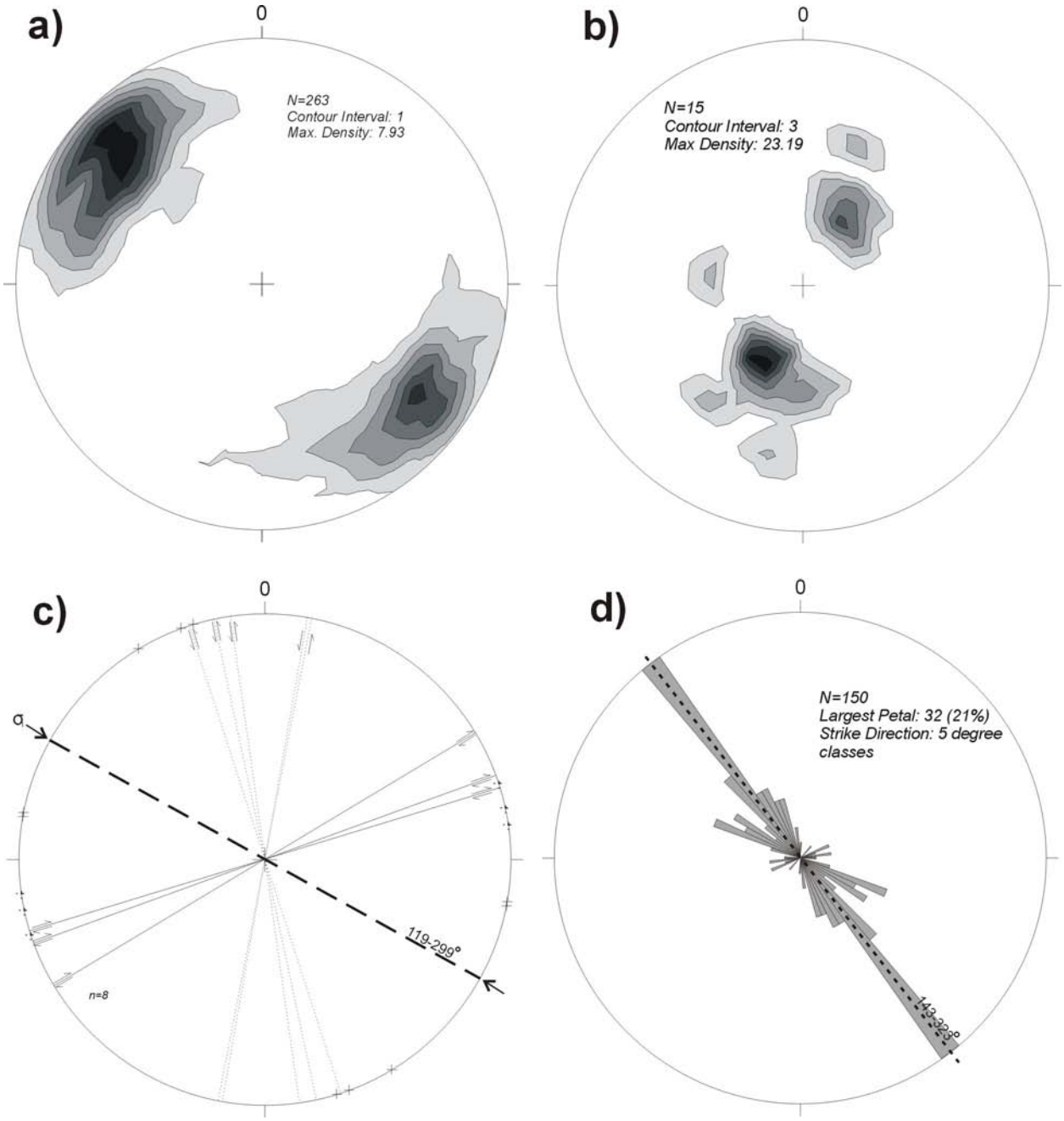

Figure 6 - a) Poles to S_2 foliation; b) F_2 fold axes; c) stereographic plot of late-D_2 dextral and sinistral shear planes with estimated orientation of main compressive stress (σ_1) during late-D_2; and d) rose diagram of late fractures illustrating a dominant orientation of 143º to 323º.

trending dextral shears and imply that the main compressive stress (σ_1), during the time of D_2 discrete shear zone development, was oriented west-northwest–east-southeast.

At Hoidas Lake and locally towards the east, individual mylonite zones range from metres to hundreds of meters in width and are characterized by widespread grain-size reduction and recrystallization, unit attenuation, quartz ribboning, and leucosome dismemberment. Mylonitization is exemplified along the western shore of Hoidas Lake in granitic gneisses which display strong quartz ribboning and locally a well developed stretching lineation that plunges moderately to steeply to the east-southeast (Figures 8 and 9). Shear zones are parallel to S_2, and are interpreted as being part of one progressive episode. Shearing formed rare δ-porphyroclasts and back-rotated boudins indicating a dextral sense of movement in the mylonite zones. The moderate to high plunge-angle of the stretching lineations, however, suggests that there is a high degree of oblique-reverse movement on the shear zones.

Although kinematic indicators are rare, the inferred dextral sense of shear is consistent with previous findings for early ductile movement along the Black Bay Shear Zone (Ashton *et al*., 2001).

c) D_3 Deformation

Gentle folding of previous structures about F_3 fold axes resulted in the minor reorientation of the $S_0/S_1/S_2$ fabric. The rare F_3 folds are moderately south to southwest plunging and are distinguished from D_2 structures by their open interlimb angles and lack of an axial planar foliation.

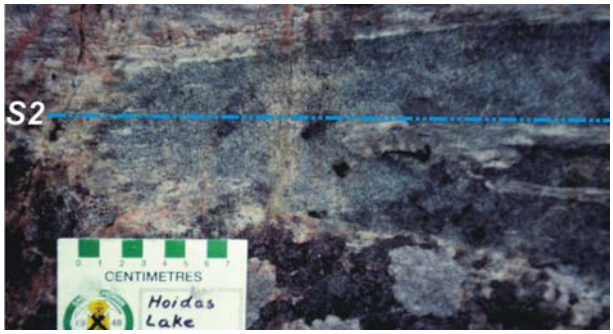

Figure 7 - Tight to isoclinally folded (F_2) amphibolitic inclusion in tonalitic gneiss east of Hoidas Lake. Note axial planar S_2 foliation.

Figure 8 – Heterogeneously strained medium-grained pink tonalitic gneiss. Note fine-grained mylonitic zone on the left of the photo. Outcrop is east of Hoidas Lake.

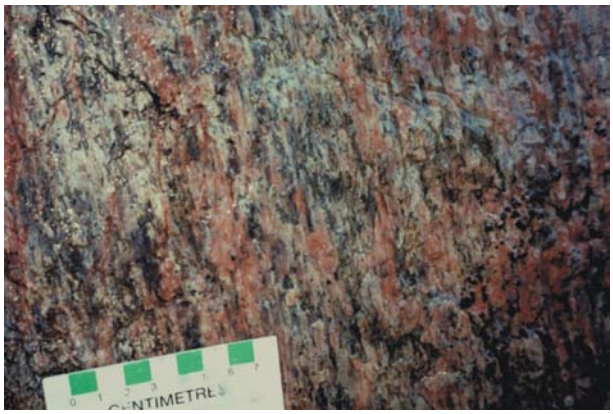

Figure 9 - A well developed mineral stretching lineation developed on the S_2 foliation plane of a mylonitic granitic gneiss at the south end of Hoidas Lake.

d) Late Faults and Lineaments

There are three dominant orientations of brittle faults (Figures 2 and 10): east, southeast, and northeast. The east-trending set is broadly parallel to the Tazin River Fault, 15 km southwest of the study area (Figure 1). The Tazin River Fault, as described by Koster (1965a, 1965b), is a brittle structure associated with quartz veining that, in the Burchnall Lake area to the west, crosscut the Martin Formation (Koster, 1970). At Hoidas Lake, the east-trending fault through the western and eastern bays of the lake is sub-parallel to the Tazin River Fault and probably part of the same fault set. Additionally, like the Tazin River Fault, it contains pervasive quartz and epidote veins at the west end of the western bay. The southeast-trending set of faults is generally oriented 30º from the east-trending set. Although relatively uncommon in the map area, this set of faults is accompanied, at outcrop scale, by a pervasive sub-vertical set of extension fractures that strike 143º (Figure 6d). These fractures are commonly associated with hematization of adjacent units.

The third set of faults trends northeasterly, sub-parallel to the Black Bay Fault. They commonly overprint older ductile high-strain zones. An example is the Nisikkatch–Hoidas Lakes Fault, which is superimposed on a D_2 mylonitic zone. This is similar to the Black Bay Fault, a brittle fault zone which overprints mylonites of the Black Bay Shear Zone (Koster, 1965a). Apart from the main fault, there are a number of smaller discontinuous splay faults which lack a recognizable older ductile component and are most common immediately west of Hoidas Lake (Figure 2).

4. Rare-earth Mineralization

a) General

Prospecting has been historically concentrated along a trend extending from Nisikkatch Lake in the southwest to Oshowy Lake in the northeast (Figure 10). Allanite $(Ca, Fe^{2+})_2(Al,Ce,Fe^{2+})_3(OH)(SiO_4)_3$ showings, which were discovered in the 1950s (e.g., J. Lane; SIR Assessment File 74O13-NW-0001), flank the northeast-trending fault and extend from beyond the southern end of Nisikkatch Lake past the northern end of Hoidas Lake. Work in the 1950s resulted in at least 29 trenches along the three lakes (Figure 10) although little data remains for discussion. The discovery of the Hoidas Lake allanite showing along the northwestern edge of the lake (Jak zone) led to initial trenching and sampling which produced assay values up to 7.0% Ce, 6.0% La, 2% Th, 0.5% Y, and 0.1% Gd. In 1955, D.D. Hogarth,

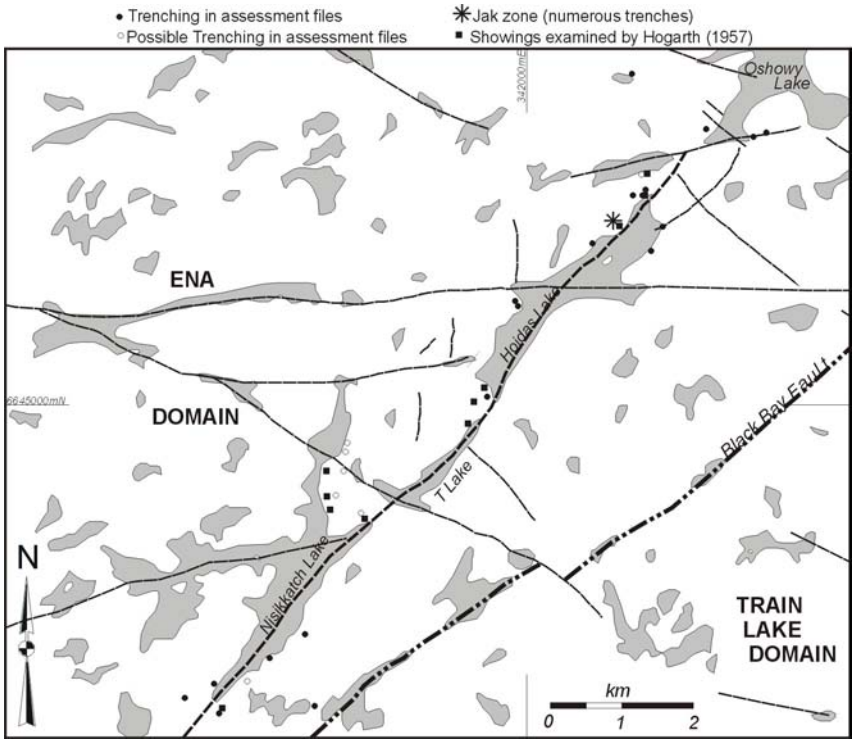

Figure 10 - Map of the Hoidas Lake area illustrating the major lineaments recognized on airphotos. Trench locations discussed in assessment files are shown as circles and showings examined by Hogarth (1957) are shown as solid squares.

from McGill University (Hogarth, 1957), examined a number of apatite- and allanite-rich veins along Hoidas and Nisikkatch lakes (Figure 10). His work defined a distinct zoning to the veins including inner zones of carbonate (calcite-barite), feldspar (hyalophane), apatite-allanite, and an amphibole-rich marginal zone (Hogarth, 1957). Total rare earth element concentrations of up to 12.03% were reported. Over the next several years, the showing was periodically examined with little progress made on understanding the geology and metallurgy of the deposit.

In 1996, Daren Industries Ltd. staked a claim covering the main Jak allanite showing along northwestern Hoidas Lake. Initial metallurgical testing revealed that it was possible to recover 97.6% of the rare-earth elements from the allanite using gravimetric separation followed by cold HCl acid leaching. In 1999, Great Western Minerals Group Ltd. optioned the Hoidas Lake property from Daren Industries and carried out a program of trenching and sampling on the Jak zone (Figure 11). This work indicated multiple horizons of allanite-bearing veins in a zone 50 to 60 m wide. Assays of grab samples returned up to 20.33% total rare earth oxides (TREO) with channel samples of individual veins containing up to 4.9% TREO over 3.2 m (Table 1).

Following this, Great Western Minerals Group Ltd. carried out a sixteen hole, 1100 m NQ drilling program on the Jak zone over a strike length of 475 m (Figure 11). Samples from this program were used to conduct extensive assaying and metallurgical testing (Table 2). The highest individual assay result was 14.11% TREO over 0.5 m from DDH 01-08. Intervals of individual veins contained up to 4.41% TREO over 6.9 m. Metallurgical testing showed

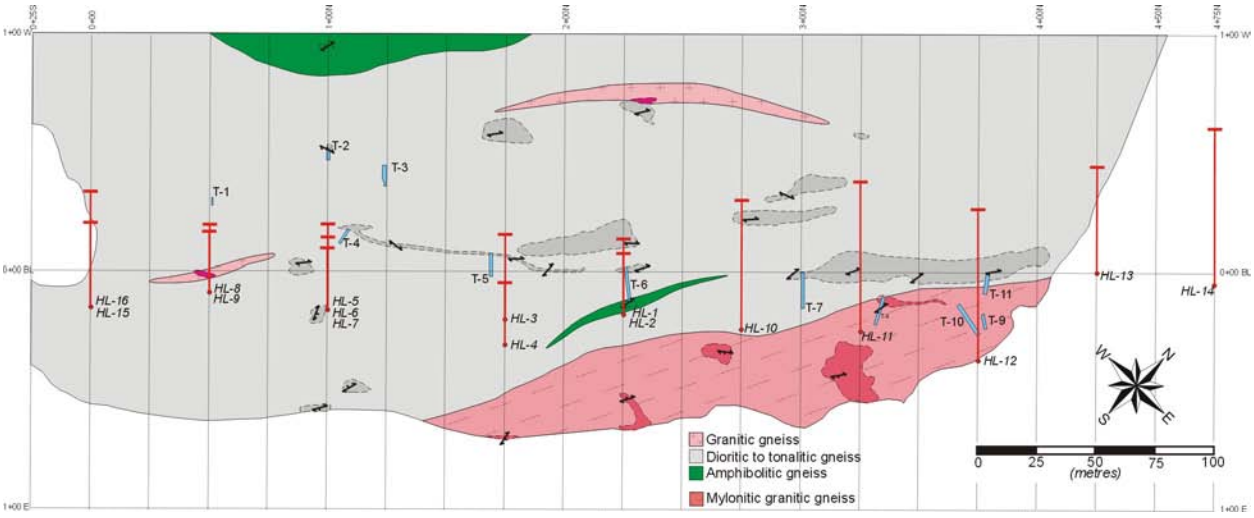

Figure 11 - Simplified geological map of the Jak zone grid, on the northwestern shore of Hoidas Lake (see Figure 2 for location; DDH locations shown as circles, trenches are prefixed with "T").

Table 1 - Total rare earth oxide analyses from chip sampled trenches with a sample spacing of approximately 0.5 m. Note TR-7 is from an old trench and only grab samples were taken.

Trench No.	Trench Width (m)	No. of Samples	# of ore veins	Average TREO	Includes (Average TREO/length)
GWG-3	5.9	10	2	1.66	5.56/1 m
GWG-4	5.4	10	2	2.717	5.42/1.3 m and 3.59/1.6 m
GWG-5	8.5	15	3	1.636	2.96/2.8 m and 3.10/0.5 m
GWG-6	13	23	4	3.301	4.02/2 m, 3.6/1.9 m, 5.14/1.2 m, 5.08/1.3 m
GWG-7	9.3	17	2	1.086	5.5/1.3 m and 3.26/1 m
GWG-8	8.4	15	3 or 4	1.01	1.81/1.1 m, 1.09/1.3 m and 6.514/0.5 m
GWG-9	3.5	7	2	1.676	5.843/0.5 m and 3.923/0.5 m
GWG-11	4.4	4	1	0.935	3.244 m
TR-7	2	2		18.477	

that up to 98.6% of the rare earth oxides could be recovered using conventional flotation and simple acid leaching methods. Further testing showed that using readily available, non-toxic reagents to leach the elements, as opposed to conventional acid leaching, recoveries close to 100% of approximately 50% of the 58 elements tested and 95 to 99% of 15 REEs and Y could be achieved.

b) Lithology

The Jak zone is underlain by two main rock types (Figures 11 and 12). Most common is fine- to medium-grained, light pink to medium grey dioritic to tonalitic gneiss that is equivalent to the tonalitic gneiss unit mapped regionally. The second unit is highly mylonitized granitic gneiss that is exposed adjacent to the northwestern shoreline along the eastern edge of the grid. Ultramylonitic textures and a strong stretching lineation are heterogeneously developed. The granitic gneiss is composed of 35 to 65% alkali feldspar, 10 to 25% quartz, 5 to 25% plagioclase, trace to 15% hornblende, 0 to 15% clinopyroxene, 0 to 5% biotite, trace to 5% allanite, along with 0 to 3% apatite and accessory epidote and sphene. As on the regional scale, attenuated schlieren and lenses are observed.

c) Mineralization

A pyroxene- and apatite-rich vein network, that is up to 60 m wide and includes two or more dominant vein horizons, hosts allanite (Figures 11 and 12). Drilling has defined a minimum strike length of 475 m; this is open at both ends. Individually, the veins vary in thickness along strike with maximum thicknesses up to 5 m. Generally, they strike northeasterly, sub-parallel to the main S_2 foliation, and dip steeply southeast although some are crosscutting (Figure 13). Veins have been intersected at depths of up to 65 m and appear to continue beyond that depth. The veins exhibit sharp contacts (Figures 13 and 14) although alteration of the adjacent country rock, characterized by slightly elevated TREO values, is not uncommon. The veins are thought to have been emplaced along northeasterly trending faults/fractures oriented sub-parallel to the S_2 foliation. Reactivation of these fault structures ranges from micro-faulting to intense vein brecciation (Figure 12b). The mineralization grades from low-grade zones in the adjacent country rock to high-grade zones in the veins.

Table 2 - Weighted average total rare earth oxides (TREO) for entire sample interval and vein-mineralized intervals. Holes are arranged from south to north. Assays are expressed as percent and include the 15 REEs (Ce, Dy, Er, Eu, Gd, Hf, Ho, La, Lu, Nd, Pr, Sm, Tb, Th, and Tm) and Y.

DDH Hole	Section (m) north	Angle	Sampled width (m)	TREO %	Vein width (m)	TREO %
15	0	45	4.9	0.63	2	2.63
16	0	65	90.4	0.27	3.5	3.59
8	50	45	24.2	1.22	4.9	4.22
9	50	65	55.8	0.64	5.2	4.62
6	100	41	23.8	0.64	3	4.5
7	100	65	37.3	0.57	4.2	4.53
3	175	45	44.1	0.48	3.4	4.38
4	175	65	35.8	0.27	2.3	3.93
1	225	45	27.9	0.32	3.3	1.16
2	225	65	36	0.47	2.3	2.62
10	275	45	12.6	1.34	1.3	3.27
11	325	45	24.1	0.73	6.7	1.88
12	375	45	68.2	0.39	2.9	3.47
13	425	50	44.9	0.67	4.9	4.3
14	475	50	66.7	0.71	6.9	4.41
		Average	39.78	0.62	3.79	3.57

In detail, two vein types are recognized in those exposed in the trenches and intersected in diamond drill core (Figure 12): 1) a pyroxene-rich zone which is dominated by clinopyroxene, scapolite, and allanite (Figure 13); and 2) an apatite-rich zone which is dominated by a red-

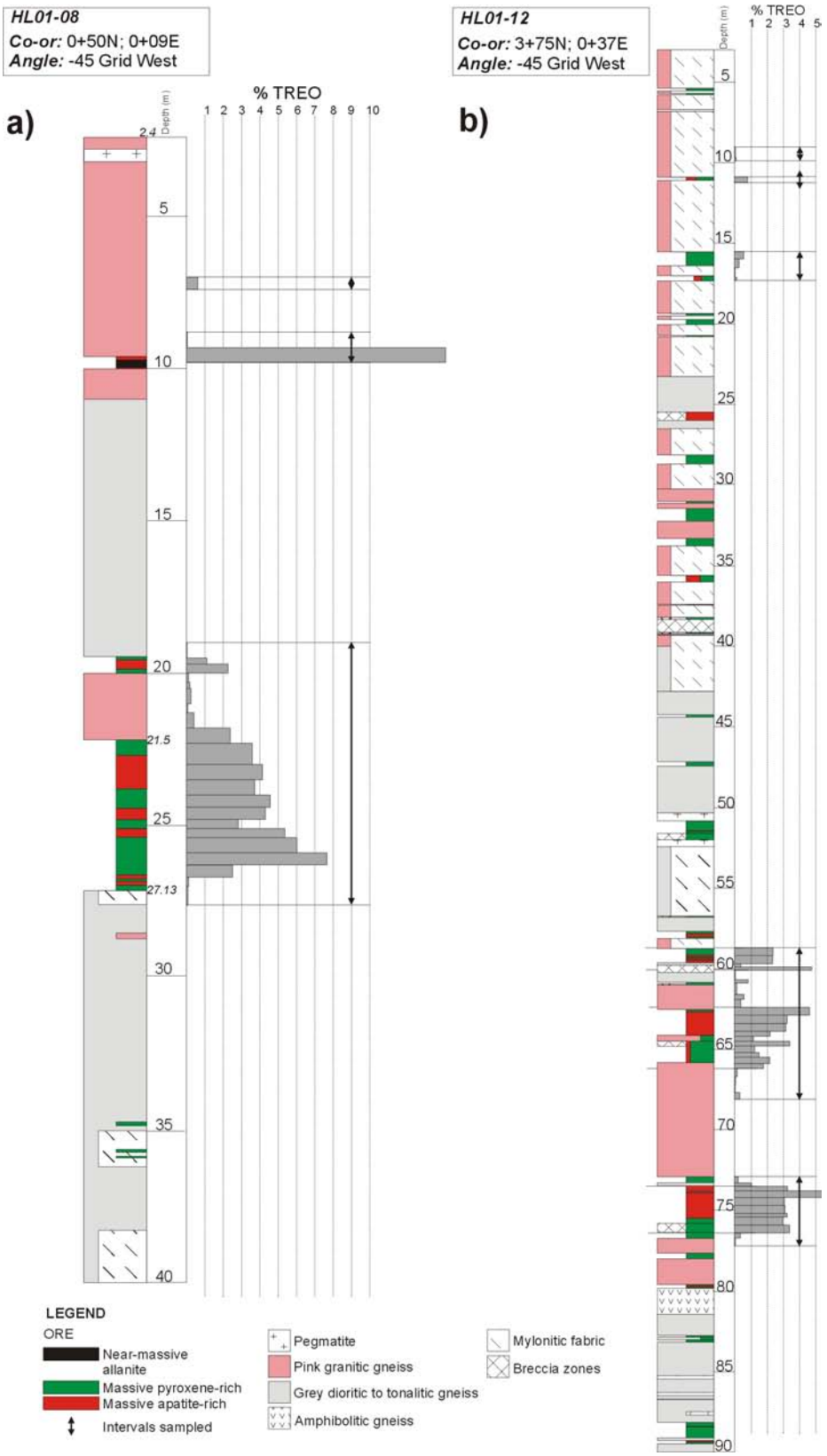

Figure 12 - NQ corehole logs from a) DDH HL01-08 and b) HL01-12 illustrating vein thickness at multiple levels.

brown apatite and allanite (Figure 15). Although end-member varieties of the two vein types are observed, it is more common to see a zonation of the two vein phases within an individual vein. The veins locally exhibit a zoning in which the margins are pyroxene rich giving way sharply to a central apatite-rich zone.

Figure 13 - Clinopyroxene-rich vein (dark green on colour photo) crosscutting the strong S_2 gneissic fabric (from trench 8).

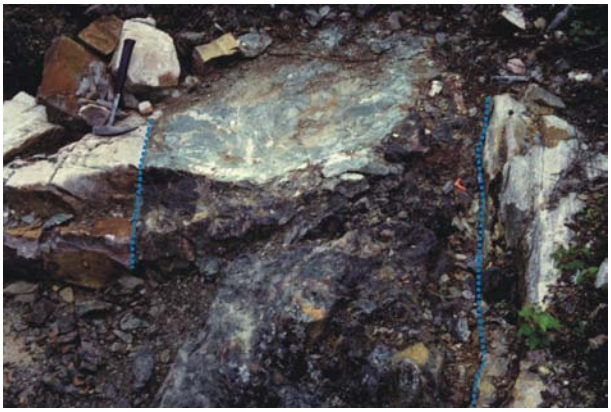

Figure 14 - Pyroxene-rich vein oriented subparallel to, and in sharp contact with, the mylonitic (S_2) granitic gneiss at trench 8.

Figure 15 - Coarse-grained vein exhibiting the relationship between the pyroxene-rich green-grey zone (cpx-scapolite-allanite) and apatite-rich red-pink zone (apatite-allanite).

Pyroxene-rich Zone

The pyroxene-rich zone is composed of 40 to 65% clinopyroxene, variably altered 0 to 40% scapolite, 5 to 50% allanite, 0 to 30% amphibole, trace to 3% zircon, and trace to 1% epidote. Amphibole grains are typically in clinopyroxene and biotite locally occurs as centimeter-scale books. Based on birefringence, scapolite is deemed to be a calcium-enriched variety (mizzonite). In fresh samples, the rock is typically dark green with subordinate interstitial red zones dominated by scapolite. The pyroxene-rich phase occurs in veins both by itself and intermixed with the apatite-rich phase. Individual pyroxene-rich veins are common in core as 0.5 cm to 3 m thick zones exhibiting sharp contacts with the surrounding rock. The chemical composition of the pyroxene-rich zone is summarized in Table 3 and illustrates elevated values of cerium and neodymium, even in these relatively allanite-free samples.

Apatite-rich Zone

The apatite-rich zone is composed of 75 to 90% red-brown apatite ($Ca_5(PO_4)_3(F,Cl,OH)$), trace to 10% hornblende, 5 to 35% allanite, trace to 4% calcite, and trace chlorite and zircon. Apatite grain size is bimodal: a common coarse population with grains up to 5 cm long (averaging 2 to 6 mm) and a very fine-grained population (<0.25 mm) confined to thin (<1 mm) micro-fault zones. The finer population was derived from recrystallization of the coarser grains. Larger apatite grains typically contain elongate inclusions oriented along the weakly developed cleavage traces. Allanite grains occur both as “fresh” and metamict forms. Non-metamict grains are typically browny orange with a low birefringence (up to 0.03). In contrast, the metamict variety, formed via destruction of the crystalline structure by the bombardment of α-particles emitted by the radioactive constituents (Deer *et al*., 1992), are dark yellow brown exhibiting a very low birefringence (effectively isotropic). Intense radial fracturing is common in adjacent minerals. Although allanite generally ranges in concentration from 5 to 35%, it locally reaches up to 70% in near-monometallic zones (Figures 12a and 16). Calcite is locally present in the apatite-rich zones, particularly in brecciated varieties. It also occurs in late crosscutting veins. The apatite-rich zone contains approximately 34% P_2O_5 and 50% CaO, as well as elevated concentrations of REE, particularly lanthanum, cerium, praseodymium, neodymium, samarium, gadolinium, and dysprosium.

Local fault zone reactivation after emplacement of the veins created structures ranging from micro-faults with resultant grain size reduction of apatite, to breccias. Alteration is associated with these late structures. Although observed in both zones, this reactivation is best expressed in the apatite-rich zone where sparsely dispersed, sub-rounded grains of apatite are rimmed by

Table 3 - Major oxide and some trace element analyses for mineralized veins from Hoidas Lake. Samples 12-25.5 and 12-75.0 are predominantly from the apatite-rich zone, whereas 12-32.0, T11, and 12-75.5 are from the pyroxene-rich zone (samples from UTM 343530; 6647580 NAD27).

		Sample Number				
		12-25.5	**12-75.0**	**12-32.0**	**T11**	**12-75.5**
SiO_2	%	4.27	4.84	44.83	50.3	43.26
Al_2O_3	%	0.29	0.21	7.81	7.46	8.11
Fe_2O_3	%	1.22	1.85	12.6	9.55	12.01
MgO	%	0.56	1.06	11.24	8.09	13.46
CaO	%	50.78	51.18	16.61	16.59	14.15
Na_2O	%	0.07	0.1	0.97	0.81	0.53
K_2O	%	0.03	0.04	1.17	2.17	1.63
TiO_2	%	< .01	0.01	0.77	0.39	1.21
P_2O_5	%	37.77	34.4	0.06	0.05	0.15
MnO	%	0.07	0.08	0.37	0.37	0.34
Cr_2O_3	%	< .001	< .001	0.005	0.006	0.006
Ba	ppm	349	2620	1935	14998	11739
LOI	%	1.8	2.2	2.9	1.1	3.4
TOT/C	%	0.17	0.44	0.11	0.04	0.03
TOT/S	%	0.14	0.38	0.1	0.01	0.02
SUM	**%**	**96.91**	**96.27**	**99.56**	**98.57**	**99.57**
Sr	ppm	8886.7	13311.5	1585	4876.1	1630.1
Th	ppm	595.1	454.7	19.6	245.3	6.7
U	ppm	96.3	81.1	2.4	7.8	2.1
Zr	ppm	13.2	71.4	196.5	118.2	229.4
Y	ppm	819.8	665.8	50.2	48.8	33.5
La	ppm	4083.6	4655.8	264.4	1885	224.6
Ce	ppm	10404.7	10857.8	568.3	3389.3	454.1
Pr	ppm	1590.91	1664.93	74.96	418.47	61.55
Nd	ppm	7016.3	6685.9	311.2	1292.8	251
Sm	ppm	1238.4	1110.6	58.8	131.8	43.1
Eu	ppm	308.8	267.88	15.91	26.97	10.1
Gd	ppm	563.72	456.84	31.23	29.01	21.45
Tb	ppm	56.74	46.53	3.31	3.87	2.16
Dy	ppm	202.85	166.57	12.75	13.89	8.22
Ho	ppm	22.35	17.83	1.6	1.17	0.92
Er	ppm	45.99	34.66	3.37	2.44	2
Tm	ppm	5.82	4.65	0.44	0.43	0.28
Yb	ppm	33.59	26.41	2.56	2.75	1.73
Lu	ppm	4.14	3.36	0.4	0.38	0.27

Figure 16 - Apatite-rich vein associated with dark black allanite from trench 8.

a very fine-grained, highly altered zone of apatite, calcite, hornblende, and hematite. In highly brecciated versions, calcite and hematite can constitute up to 50% of the rock.

5. Summary

In general, granitic and tonalitic gneisses that intrude an older package of amphibolite are the main units in the Hoidas Lake area. These rocks are heterogeneously strained and locally mylonitic. Late intrusive units include weakly to moderately foliated garnetiferous dioritic gneiss and massive granitic pegmatites.

Two prominent deformation events were followed by a weaker one. D_1 is characterized by the transposition of primary layering observed in the amphibolitic unit, into the locally preserved S_1 foliation. S_1 is parallel to the axial planes of rare F_1 isoclinal folds. D_2, the dominant event in the Hoidas Lake area, formed tight to isoclinal F_2 folds and a variably intense foliation ranging from weak to mylonitic. Northeast-trending D_2 mylonite zones, which range from a few metres to hundreds of metres wide, are associated with, and are sub-parallel to, the long-lived Black Bay Shear Zone to the east. The widest mylonite zone is coincident with the long axis of Hoidas Lake. Moderately east-southeast plunging stretching lineations, together with rare kinematic indicators, suggest an oblique-reverse dextral sense of movement on the D_2 shear zones. Post-D_3 brittle to possibly brittle-ductile faults are defined by lineaments in three main trends. The most important are the northeast-trending ones superimposed on earlier D_2 structures (e.g., the Nisikkatch-Hoidas Lakes Fault). These faults and associated splay fractures appear to be most common immediately west of Hoidas Lake.

The Hoidas Lake REE deposit is in pyroxene- and apatite-rich veins in northeast-trending brittle to brittle-ductile faults that are sub-parallel, and likely related, to the Black Bay Fault 3 km to the east. Reactivation of these fault structures has resulted in localized brecciation of the mineralized veins. Two end-member vein types host the rare-earth-bearing minerals, with variably zoned combinations being most common. Mafic pyroxene-rich veins are composed mostly of clinopyroxene with subordinate scapolite and allanite. In contrast, the apatite-rich veins consist of over 70% apatite, with subordinate clinopyroxene, allanite, and

amphibole. In concert, these phases form complexly zoned veins with total rare-earth element oxides up to 4.4% over 6.9 m. The vein network encompasses a width of up to 60 m, has a drill defined strike length of 475 m, and remains open at both ends and at depth.

Determination of the paragenesis of the vein network requires further petrographic and geochemical analyses. The working model is that late veins of possible ultramafic to lamprophyric composition were emplaced along post-D_3 faults and fractures and subjected to further metamorphism/metasomatism. A common method to produce Ca-rich scapolite is to subject a pyroxene-plagioclase-rich rock to a calcite-rich fluid resulting in Ca-rich scapolite becoming the stable aluminosilicate instead of plagioclase (Deer *et al*., 1963). In addition, according to Deer *et al*. (1962), chlorapatite may be associated with scapolite in rocks that have undergone chlorine metasomatism, although further work is required to test apatite composition.

Apart from the Uranium City area, much of the region north of Lake Athabasca is largely underexplored. Early work indicated a spatial relationship between rare-earth element occurrences and late northeast-trending faults. The close proximity and similar history, involving early ductile movement and later brittle-ductile to brittle faulting of the Nisikkatch-Hoidas Lake Fault and the Black Bay Fault suggests a genetic relationship. This relationship, and the abundance of apparently similar allanite-bearing quartzofeldspathic gneisses immediately west of the Black Bay Fault, suggests the potential for further REE discoveries not only in the eastern Ena Domain, but in other domains to the southwest.

The primary vein network may be part of a larger event coincident with the intrusion of late ultramafic bodies throughout the south-southeastern Ena Domain. Work by Koster (1965a, 1965b, 1970) briefly mentions the presence of peridotite and pyroxenite dykes up to 30m thick in an area within approximately 5 km of the Black Bay Fault and within 2.5 km of the Tazin River Fault to the southwest, a strike distance of over 50 km. These bodies appear to be most common along the western edge of Nisikkatch Lake and towards the southwest. In the Nisikkatch Lake area, the ultramafic bodies have a northeasterly trend and are oriented sub-parallel to the Nisikkatch-Hoidas Lakes Fault and the Black Bay Fault, perhaps indicating a similar history to the mineralized veins along Hoidas and Nisikkatch lakes. A large system capable of such widespread intrusive activity would have had the potential to leach REE from surrounding country rock. To this end it is important to note that allanite is not only present in the Hoidas Lake area, but also in the host rocks of the Black Bay Fault south to Lake Athabasca (Ashton *et al*., 2001). The recognition of relatively late clinopyroxene-rich dykes infilling brittle-ductile to brittle faults associated with the Black Bay Fault or other faults may be the key to further discoveries.

6. Acknowledgments

Mark Urban provided tireless and able assistance both in office and field. Thomas Love, Peter McPherson, and Ken Tong provided invaluable computer-based assistance. Review and critical comments by Saskatchewan Industry and Mines staff are greatly appreciated.

7. References

Alcock, F.J. (1936): Geology of Lake Athabasca Region, Saskatchewan; Geol. Soc. Can., Mem. 196, 41p.

Ashton, K.E., Boivin, D., and Heggie, G. (2001): Geology of the Black Bay Belt, west of Uranium City, Rae Province; *in* Summary of Investigations 2001, Volume 2, Saskatchewan Geological Survey, Sask. Energy Mines, Misc. Rep. 2001-4.2, CD A, p50-62.

Bucher, K. and Frey, M. (1994): Petrogenesis of Metamorphic Rocks, 6th edition; Springer-Verlag, Berlin, 318p.

Deer, W.A., Howie, R.A., and Zussman, J. (1962): Rock Forming Minerals: Volume 4, Non-Silicates; John Wiley and Sons Inc., New York, 371p.

_____ (1963): Rock Forming Minerals: Volume 4, Framework Silicates; Longmans, London, 435p.

_____ (1992): An Introduction to Rock-forming Minerals (2nd edition); Longman Scientific and Technical, Essex, 696p.

Hogarth, D.D. (1957): The apatite bearing veins of Nisikkatch Lake, Saskatchewan; Can. Mineral., v6, p140-150.

Koster, F. (1965a): The Geology of the Dardier Lake Area (west half); Sask. Dep. Miner. Resour., Rep. 101, 45p.

_____ (1965b): The Geology of the Ena Lake Area (east half); Sask. Dep. Miner. Resour., Rep. 91, 31p.

_____ (1970): The Geology of the Burchnall Lake Area; Sask. Dep. Miner. Resour., Rep. 131, 24p.

Macdonald, R. (1983): Geology and regional context of the Oldman Lake area; *in* Summary of Investigations 1983, Saskatchewan Geological Survey, Sask. Energy Mines, Misc. Rep. 83-4, p19-23.

Slimmon (1989): Compilation Bedrock Geology, Fond-du-Lac, NTS Area 74O; Sask. Energy Mines, Rep. 247, 1:250 000 scale map with marginal notes.